



## Planning and processing of Zn-Ni alloy thin film by electrodeposition

Hawa Bendebane<sup>1,2,\*</sup>, Salima BENDEBANE<sup>3,4</sup>, Samia AMIRAT<sup>1,2</sup> Rabah REHAMNIA<sup>1,2</sup>

<sup>1</sup> Department of Chemistry University of Badji-Mokhtar of Annaba, Algeria

<sup>2</sup> Laboratory LNCTS

<sup>3</sup> Higher National School of Technology and Engineering

<sup>4</sup> Laboratory LOMOP

Received: 6 January 2023; Revised: 5 August 2023; Accepted: 19 September 2023

\*Corresponding author e-mail: bendebanehawa@yahoo.fr

**Citation:** Bendebane, H.; Bendebane, S.; Amirat, S.; Rehamnia, R. *Int. J. Chem. Technol.* 2023, 7 (2), 162-170

### ABSTRACT

Electrodepositions of zinc-nickel alloy thin films on Low-carbon steel from sulfate acid baths were studied. An experimental design and optimization procedures for Zn-Ni alloy electroplating was applied using Minitab 19. This paper analyzed a six-variable in two steps. (1) A Mixture Design (MD) where the best proportion between boric acid, saccharin, and 2-butyne-1,4-diol was determined. (2) Box Behnken design to find the most optimal conditions for zinc-nickel electroplating. For that temperature, current density, and the ratio  $[Ni^{2+}]/[Zn^{2+}]$  are the tested parameters. In step 1 the best bath composition was  $[boric\ acid] = 0.1M$ ,  $[saccharin] = 0.3\ g/L$ , and  $[2-butyne-1,4-diol] = 0.1\ g/L$ . It was found, from step 2, that the best coating in terms of quality, brightness, and hardness was obtained under the following conditions:  $T = 30^{\circ}C$ ;  $i = 0.5A/dm^2$  and  $[Ni^{2+}]/[Zn^{2+}] = 0.53$  with a theoretical response of 312.66 HV and an experimental response of 312.30 HV. These results were confirmed by two analyses morphological (SEM) and elemental (EDS).

**Keywords:** Electrodeposition, Zn-Ni alloy, thin film, experimental design, mixture design, Box-Behnken, microhardness.

### 1. INTRODUCTION

Surface treatment by coating is a technique more and more used. It consists of improving surface properties by means of a film in order to give the metal certain surface properties such as corrosion resistance, appearance (bright, matte, semi-gloss....), and optical properties<sup>1-3</sup>. Since zinc-based alloy coatings are more corrosion resistant than pure zinc coatings<sup>4,5</sup>, zinc-nickel coatings have long provided better corrosion protection for steel<sup>6,7</sup> because of their excellent corrosion resistance, hardness, non-toxicity, and thermal stability<sup>8,9</sup>. Therefore, these coatings are frequently used in industries<sup>10, 11</sup>. And to achieve this type of alloy a simple, easy and especially economical method has been considered. This method is electrodeposition<sup>12</sup>.

In the context of creating a barrier between the metal and the corrosive environment by applying the

electrodeposition method, several objectives were aimed in this study.

To find the critical electrodeposition variables affecting the micro-hardness of Zn-Ni deposits, a two-step experimental design was developed. The results of each step were used to determine the optimum conditions for Zn-Ni electrodeposition.

Step 1: Mixture design (MD): it was used to provide maximum information on the constituents, their individual be planned and facilitated<sup>13,14</sup>. The aim is to obtain mixture with optimum response or meet certain requirements set from the outset. The desired response depends on the proportions of the constituents used. Thus, for a mixture with three proportions (sodium citrate, saccharin, and 2-butyne-1,4-diol), their sum is equal to unity, which means that they are dependent on each other.

Step 2: Box-Behnken design: Once the best bath composition had been determined, experimental planning was carried out with the aim of improving coating quality. The deposition was carried out using the Box-Behnken design. To achieve this, we chose three different factors such as current density ( $i$ ), bath temperature, and  $[Ni^{2+}]/[Zn^{2+}]$  ratio.

Step 3: Analysis techniques: the optimized samples in steps 1 and 2 were analyzed by using Scanning electron microscopy (SEM) and energy dispersive spectroscopy (EDS). The SEM was used to analyze the microstructure of the Zn - Ni deposits. Moreover, EDS was used to measure the chemical composition of the optimized samples.

## 2. MATERIALS AND METHODS

### 2.1. Working electrode

Low-carbon steel substrates, conforming to SAE 1010, ASTM A-366, and QQS-698 were used in this study. The chemical composition of the main principal elements of the substrate was represented in Table 1. The substrate requires adequate surface preparation to remove any

impurities present at the interface. This preparation was presented in manual polishing and chemical attacks which are the classical techniques of substrate preparation. Indeed, the polishing was done with an abrasive paper of grade 800 to grade 2000, and to eliminate any impurity on the surface an attack with ethanol and HCl (50%) was examined. Finally, the substrate was rinsed thoroughly with distilled water and then dried.

**Table 1.** Chemical composition of the substrate.

Element	C	Mn	P	S	Fe
% max	0.13	0.60	0.40	0.05	The rest

### 2.2. Electrolytes

The electrodeposition of the Zn-Ni alloy coatings was performed in a sulfate acid bath. The composition of the baths and the operating parameters kept constant in this study are shown in Table 2. Under these conditions, the pH of the solution is between 2.3 and 2.5. Each experiment was performed in fresh solution to avoid problems such as depletion of metal ions from the electrolyte.

**Table 2.** Bath compositions.

Parameters	Minimum value	Maximum value
Part1: mixture design		
Saccharin (g/L)	0.1	0.3
2-butyne-1,4-diol (g/L)	0.1	0.3
Boric acid (mol/L)	0.1	0.3
Part 2: Box-Bhenken design		
T (°C)	30	60
$i$ (A/dm <sup>2</sup> )	0.5	1.5
$[Ni^{2+}]/[Zn^{2+}]$	0.5	1.5
Fixed parameters	w: 300 rpm; Velectrolyte: 100 mL; e = 15 $\mu$ m; [Na <sub>2</sub> SO <sub>4</sub> ] = 0.40 M; [H <sub>2</sub> SO <sub>4</sub> ] = 0.01 M; [ZnSO <sub>4</sub> .7H <sub>2</sub> O] = 0.1M; Distilled water	

### 2.3. Two-electrode system method

We have tried to realize thin films of Zn-Ni alloy by the galvanostatic method. This method consists in applying a current density fixed according to the Faraday law. Samples were obtained from different baths. The cathode was the substrate and the anode was zinc. The formation of the deposit is done by a redox reaction.

At the anode:  $Zn \rightarrow Zn^{2+} + 2 e^{-}$

At the cathode:  $Zn^{2+} + 2 e^{-} \rightarrow Zn_{\downarrow}$

$Ni^{2+} + 2 e^{-} \rightarrow Ni_{\downarrow}$

For the measurement of the hardness of the obtained coatings, an INNOATEST microdurometer is used.

## 3. RESULTS AND DISCUSSION

### 3.1. Mixture design

The matrix of experiments; called the axial matrix, is presented in Table 3. It consists of ten experiments performed under the following conditions: T =30°C,  $i$  =

1 A/dm<sup>2</sup>, e = 15 $\mu$ m, t = 52mn. The last two columns represent respectively the experimental and theoretical response (the micro-hardness).

#### 3.1.1 Simplex plot

Figure.1 represents the points of the experiment carried out by the mixture design. The points are distributed at the vertices, in the middle of the stops, and in the middle of the triangle.

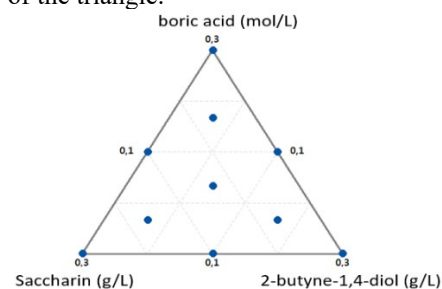


**Figure 1.** Simplex plot for the mixture of boric acid, saccharin and 2butyne1,4diol.

### 3.1.2. Henry's line

Henry's line is used to check the normality of the model because models can be difficult to interpret if the amount of data is not large. It can be seen that the points tend to form a straight line.

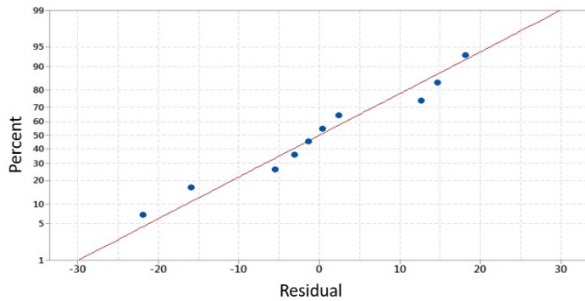


Figure 2. Henry's line for the mixture of boric acid, saccharin, and 2butyne1,4diol.

### 3.1.3. Cox diagram

This curve consists in representing the variation of the response along each Cox axis. The different curves are calculated point by point from the previously determined mathematical model and using the MINITAB 19 software. Figure 3 illustrates the variation of the micro-hardness along the Cox axes, starting from the center of gravity of the triangle taken as a reference mixture. It can be seen that for an equal composition of the three constituents, the micro-hardness decreases with the increase in the variation of the proportion of saccharin compared to the reference mixture. On the other hand, the increase of boric acid and 2butyne-1,4diol indicates an increase in micro-hardness. But beyond the reference line of the mixture, we observe a decrease of the micro-hardness with the increase of boric acid and 2butyne1,4diol. As for saccharin, a proportional relationship with micro-hardness is observed.

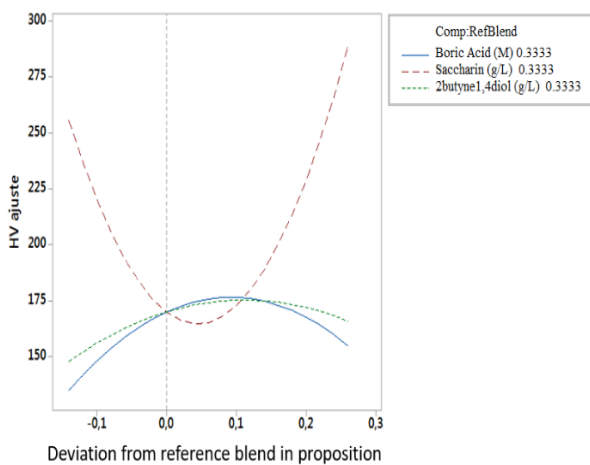


Figure 3. Cox plot for the mixture of boric acid, saccharin, and 2butyne1,4diol.

### 3.1.4. Mathematical model

The mathematical model applied to the response (micro-hardness of Zn-Ni coating) is a quadratic model for three components with a total of six coefficients for a single response according to equation 1.

$$\begin{aligned}
 HV &= -150.89 \times [Boric\ acid] \\
 &+ 2389.11 \times [Saccharin] \\
 &+ 89.11 \times [2butyne1.4diol - 7502.53] \\
 &\times [Boric\ acid] \times [Saccharin] \\
 &+ 8971.57 \times [Boric\ acid] \times [2butyne1.4diol] \\
 &- 9310.71 \times [Saccharin] \\
 &\times [2butyne1.4diol]
 \end{aligned}
 \tag{eq. 1}$$

### 3.1.5. Response Surface Methodology (RSM)

The simplex method supposes that the system studied can be represented on a response surface, limited to a specific experimental domain.

Figure 4 represents the contour plot and response surface plot of microhardness as a function of the three components (boric acid, saccharin, and 2butyne1,4diol). The gray contour located at the maximum level for saccharin (0.3g/L), the minimum level for boric acid (or the minimum level for 2butyne1,4diol) of the triangle represents the area where we have a good micro-hardness (HV > 275). The response surface represented in a polyhedron (Figure 4) is a convex shaped triangle. We can see that the micro-hardness is good at the left vertex of the polyhedron. It increases with the decrease of boric acid and 2butyne-1,4diol and the increase of saccharin.

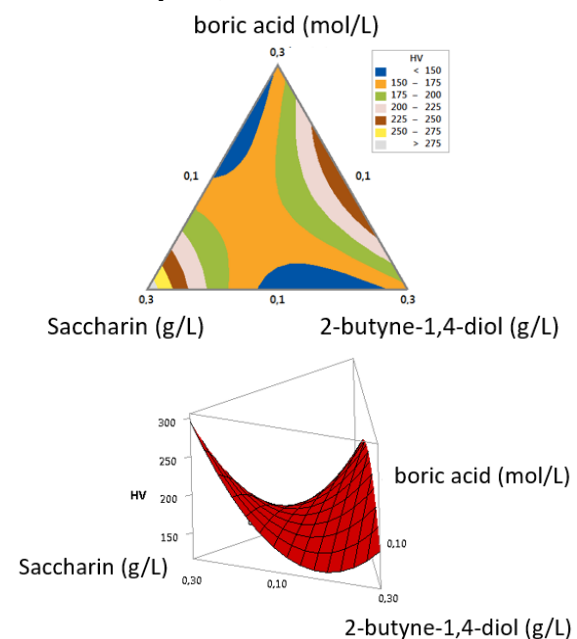


Figure 4. Response surface and contours of the mixture of boric acid, saccharin, and 2butyne1,4diol.

### 3.1.6. Optimization

To achieve the main objective of the mixture design which consists in finding the optimal mixture combining all the desired properties a statistical treatment of the

mathematical model obtained from experimental results was carried out. Indeed, a constraint was imposed on the selected factors. Table 4 summarizes the optimal conditions obtained for the tested composition.

**Table 4.** Optimal conditions for the mixture of boric acid, saccharin, and 2butyne1,4diol.

Optimal composition			Theoretical responses (HV)	Experimental responses (HV)
boric acid (M)	Saccharin (g/L)	2butyne1,4diol (g/L)		
0.1	0.3	0.1	295.88	298.20

### 3.2. Optimization of the Zn-Ni alloy electrodeposition by the Box-Behnken design

After determining the right composition of saccharin, boric acid, and 2butyne1,4diol mixture another experimental planning was carried out with whose objective is to improve the quality of coatings. The deposition was carried out by applying the response surface methodology where the Box- Behnken design

was used. For this, we chose three factors to vary such as current density (I), temperature, and the ratio [Ni]/[Zn]. Table 5 represents the experimental matrix of the different tests as well as the experimental and theoretical responses (the micro-hardness).

Working conditions: Boric acid = 0.1 M, Saccharin = 0.3 g/L, 2butyne1,4diol = 0.1 g/L,  $e = 15\mu\text{m}$

**Table 5.** experimental matrix of the different tests.

Standard order	T (°C)	i (A/dm <sup>2</sup> )	[Ni]/[Zn]	Experimental microhardness (HV)	Theoretical microhardness (HV)
14	45	1.0	1.0	163.4	163.033
12	45	1.5	1.5	115.3	125.400
1	30	0.5	1.0	304.0	298.475
9	45	0.5	0.5	253.6	243.500
13	45	1.0	1.0	162.8	163.033
5	30	1.0	0.5	179.2	194.825
11	45	0.5	1.5	162.8	168.850
6	60	1.0	0.5	149.8	150.325
7	30	1.0	1.5	184.2	183.675
10	45	1.5	0.5	108.8	102.750
2	60	0.5	1.0	160.4	169.975
4	60	1.5	1.0	141.5	147.025
15	45	1.0	1.0	162.9	163.033
3	30	1.5	1.0	146.8	137.225
8	60	1.0	1.5	125.1	109.475

#### 3.2.1. Analysis of variance

From the analysis of the variance (ANOVA) Table 6, it can be seen that a good regression of the model was obtained with a value of  $P = 0.002$ . In addition, it was found that the linear values ( $P = 0.001$ ) and the interactions ( $P = 0.010$ ) were significant. Concerning the linear terms, it was found that the current density is a highly significant parameter in the electrodeposition process with a zero  $P$  value. In addition, temperature and [Ni]/[Zn] ratio were also found to be significant factors with  $P$  values of 0.002 and 0.049 respectively.

There are also two significant interactions between  $T \times I$  and between  $I \times [\text{Ni}]/[\text{Zn}]$  with  $P$  values of 0.005 and 0.019 respectively.

#### 3.2.2. Mathematical model

The mathematical model is of second order linking the micro-hardness to the different factors, their squares, and their interaction. The regression of the HV response in coded units according to all terms is represented by equation 2 and in uncoded units is given by equation 3.

**Table 6.** Results of the ANOVA.

Source	DL	SomCar	ajust	CM ajust	F	P
Model	9	34964.8		3885.0	19.22	0.002
Linear	3	25361.7		8453.9	41.82	0.001
T (°C)	1	7044.8		7044.8	34.85	0.002
I (A/dm <sup>2</sup> )	1	16964.8		16964.8	83.93	0.000
[Ni]/[Zn]	1	1352.0		1352.0	6.69	0.049
Square	3	2234.1		744.7	3.68	0.097
T×T	1	558.2		558.2	2.76	0.157
I×I	1	609.3		609.3	3.01	0.143
[Ni]/[Zn]×[Ni]/[Zn]	1	916.4		916.4	4.53	0.086
Interaction of 2 factors	3	7369.1		2456.4	12.15	0.010
T×I	1	4781.7		4781.7	23.66	0.005
T×[Ni]/[Zn]	1	220.5		220.5	1.09	0.344
I×[Ni]/[Zn]	1	2366.8		2366.8	11.71	0.019
Error	5	1010.7		202.1		
Inadequate fit	3	1010.5		336.8	3259.58	0.000
Pure error	2	0.2		0.1		
Total	14	35975.5				

Regression equation in coded units

$$\begin{aligned}
 HV &= 729 - 10.52 \times T - 499.6 \times i \\
 &+ 47.3 \times (Ni^{2+}/Zn^{2+}) + 0.0546 \times T \times T \\
 &+ 51.4 \times i \times i - 63.0 \times (Ni^{2+}/Zn^{2+}) \times T \\
 &- 0.990 \times T \times (Ni^{2+}/Zn^{2+}) \\
 &+ 97.3 \times i \\
 &\times (Ni^{2+}/Zn^{2+}) \quad (eq. 2)
 \end{aligned}$$

Regression equation in uncoded units

$$\begin{aligned}
 HV &= 163.03 - 29.68 \times T - 46.05 \times i \\
 &- 13.00 \times (Ni^{2+}/Zn^{2+}) + 12.30 \times T \times T \\
 &+ 12.85 \times i \times i - 15.75 \times (Ni^{2+}/Zn^{2+}) \\
 &+ 34.58 \times T \times i - 7.42 \times T \times (Ni^{2+}/Zn^{2+}) \\
 &+ 24.33 \times i \\
 &\times (Ni^{2+}/Zn^{2+}) \quad (eq. 3)
 \end{aligned}$$

### 3.2.3. Main effect

From Figure 5, it can be seen that temperature and current density have a negative effect on the electrodeposition of Zn-Ni alloy. Where the micro-hardness decreases from 203.55 HV at 30°C to 144.2 HV at 60°C and also it decreases from 220.2 HV at 0.5A/dm<sup>2</sup> to 128.1 HV at 1.5 A/dm<sup>2</sup>. For the concentration ratio [Ni<sup>2+</sup>]/[Zn<sup>2+</sup>] we observe an almost constant level (from 172.85 to 177.4 HV) and then a decrease of the micro-hardness to a value of 146.85 HV at 1.5A/dm<sup>2</sup>.

### 3.2.4. Interaction effect

It was found an only strong interaction between temperature and current density T-i: this interaction is between 45 and 60°C at 1.25A/dm<sup>2</sup>. It also found three weak interactions between :

- T-i: between 30 and 60°C at the maximum level for i (1.5A/dm<sup>2</sup>).
- T-[Ni<sup>2+</sup>]/[Zn<sup>2+</sup>]: between 30 and 45°C at the minimum level for the concentration ratio [Ni<sup>2+</sup>]/[Zn<sup>2+</sup>] (0.5).
- I-[Ni<sup>2+</sup>]/[Zn<sup>2+</sup>]: between 0.5 and 1 concentration ratio at 60°C.

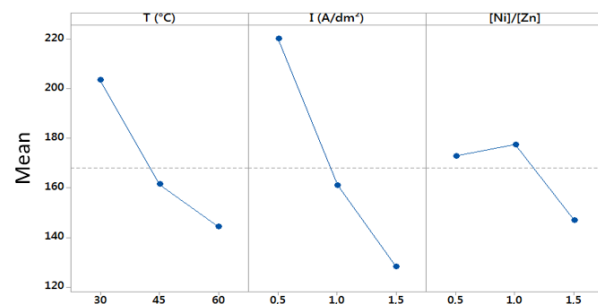


**Figure 5.** Main effect of electrodeposition of Zn-Ni.

### 3.2.5. Response and contour surfaces

Figure.7, Figure 8, and Figure 9 represent the response and contour surfaces of the micro-hardness as a function of the studied factors such as temperature, current density, and [Ni<sup>2+</sup>]/[Zn<sup>2+</sup>] concentration ratio.

For a minimum level of [Ni]/[Zn] ratio (0.5), it was observed that the best value of the microhardness (>300HV) was obtained with low values of temperature and current density. Furthermore, beyond this range, a

decrease in microhardness was observed. It was also found that the response surface is concave inclined. By fixing the current density, we found that the minimum value of I gives the best value of micro-hardness (>300 HV). The area of good microhardness is located at a minimum level for the temperature (30°C) and for a concentration ratio range of 0.5-1. The response surface has a convex shape and is slightly inclined to the left.

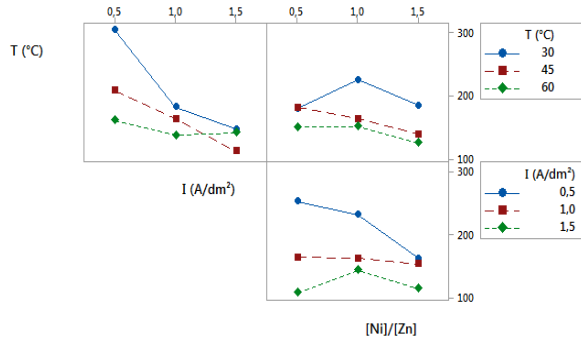


Fig. 6: Interaction effect between factors for the electrodeposition of Zn-Ni

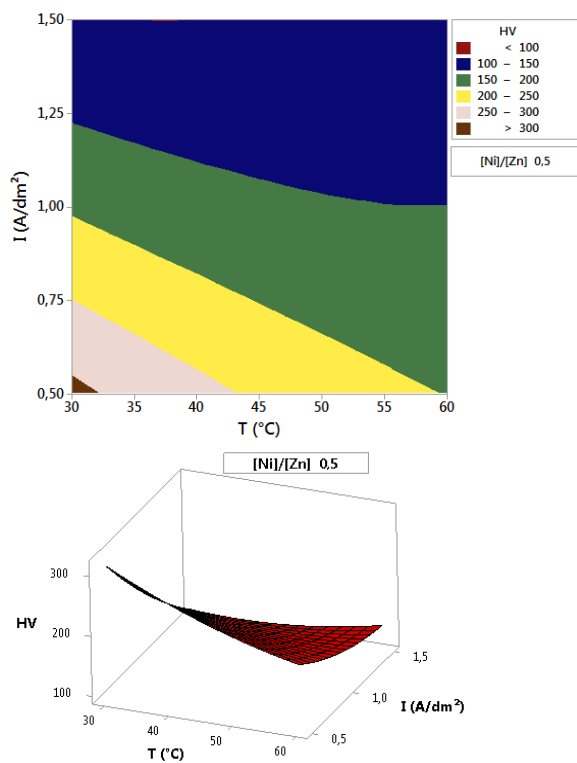


Figure 7. Contour and response surface of HV as a function of T-I at a minimum level of [Ni<sup>2+</sup>]/[Zn<sup>2+</sup>] ratio.

By fixing the temperature, it was observed that the minimum value of T gives the best value of micro-hardness (300 HV). The area of good microhardness is located at a minimum level for the current density (0.5A/dm<sup>2</sup>) and in a concentration ratio range of 0.5-1. HV. The response surface is convex and slightly inclined to the left.

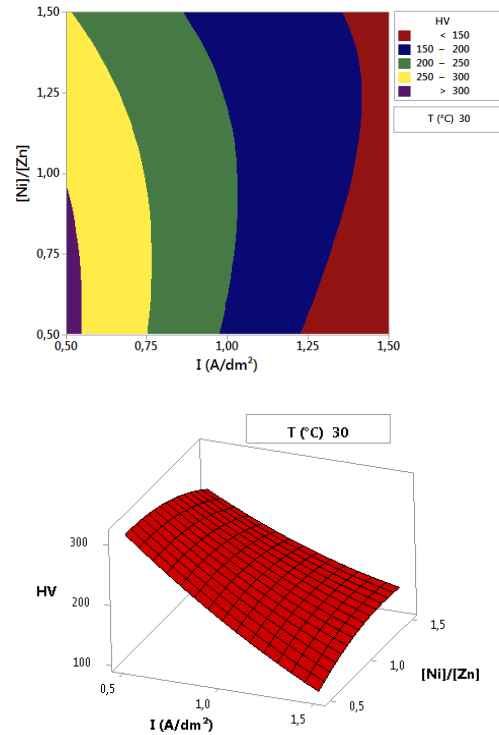


Figure 9. Contour and response surface of HV as a function of I-[Ni]/[Zn] at a minimum level of temperatures.

### 3.2.6. Optimization

In order to find the optimal operating conditions for a better coating of the Zn-Ni alloy, an optimization was examined. Indeed, a constraint was imposed on the selected factors. Figure 10 summarizes the optimal conditions obtained.

After several optimizations, the best one is given in Figure.10. The results of the optimization show the optimal values for each factor and the optimal value of the theoretical micro-hardness.

The optimal conditions are:

T = 30°C; i = 0.5A/dm<sup>2</sup> and [Ni<sup>2+</sup>]/[Zn<sup>2+</sup>] = 0.53 for a theoretical response = 312.66 HV.

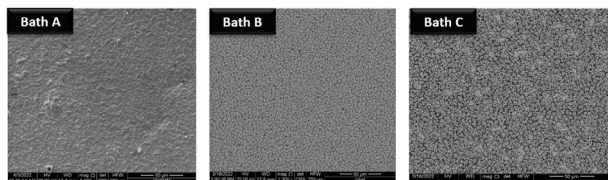


Figure.10. Optimization graph of the Zn-Ni alloy.

### 3.3. Characterization of the morphology and composition of thin films

#### 3.3.1. Scanning electron microscopy

The morphology of the coatings obtained in the absence and presence of the additives was performed by scanning electron microscopy (Figure 11). SEM images show that the composition of the bath influences the quality of the coating. Indeed, in the presence of boric acid only (bath A) a non-homogeneous surface was obtained. In contrast, the coating turned out to be more homogeneous (bath B) compared to bath A by applying a mixture design.



**Figure 11.** SEM imagery of thin film obtained in different baths.

**Table 7.** Particle sizes for the different baths.

Baths	Bath A	Bath B	Bath C
Average particle size ( $\mu\text{m}$ )	4.148	3.020	1.510

**Table 8.** Quantitative analyses (EDS) of the coatings obtained by the different baths

	Bath A	Bath B	Bath C
Zn (%)	87	90	83
Ni (%)	6	7	13
O (%)	8	3	3

### 3.4. Discussion

#### 3.4.1. Bath composition

It was found that boric acid has a significant effect on the electrochemical deposition of zinc-nickel alloy thin films. Indeed, it was observed that at lower concentrations of boric acid, a bright deposit with high micro-hardness was obtained. This result can be interpreted based on the experiments of Sachin et al.<sup>16</sup>, which show that the presence of boric acid enhances the deposition of Zn by shifting the concentration of nickel in the alloy towards the nickel-rich phases to prevent deposition. In the same finding, we find the results of Y. Tsuru et al.<sup>17</sup> who interpret the effect of boric acid on the quality of the Zn-Ni alloy formed by the significant increase of the internal stress in the nickel film.

Similarly, Lotfi et al.<sup>18</sup> reported that boric acid forms a stable complex with  $\text{Ni}^{2+}$  and acts as a homogeneous catalyst or it absorbs on the electrode surface. Similar effects of boric acid are observed by Shivakumara et al.<sup>19</sup> when depositing zinc-nickel alloys in sulfate baths. He also indicated that boric acid acts on perfect crystal growth, uniform arrangement of crystals, and refinement of crystal size.

The Zn - Ni deposits at optimum conditions of Box Behnken design (bath C) exhibited uniform, compact, and fine-grained without any pores at the surface. Based on imagej software, the measurement of grain size was performed and the results are summarized in Table 7. It was found that the grains are small in size in the order of micrometers and bath C gives the finest size. Therefore, it can be said that the thin film obtained with bath C is of smooth and glossy quality.

#### 3.3.2. Energy dispersive spectroscopy (EDS)

Table 8 summarizes the mass percentages of the different elements present in the thin film coatings formed by the three baths tested. It was found that zinc is present in the coatings formed with very high percentages (from 83 to 90%) followed by nickel with mass percentages between 6 and 13%. It was also noted that oxygen is present in these deposits with low percentage<sup>15</sup>.

The addition of saccharin to the electrodeposition bath reducing the grain size. The same observation was funding by Intan Sharhida Othman et al.<sup>20</sup>.

According to Riastuti et al.<sup>21</sup> saccharin blocks the surface of the substrates through the formation of complex compounds that effectively increase the frequency of nucleation but decreases the diffusion of ions absorbed on the cathode surface.

Since the quality of the coatings is very important in the electroplating industry, therefore the use of leveling and grain refining agents is very important. The agents commonly used are 2-butyne-1,4-diol with saccharin due to its strong inhibitory effect on the reduction of iron group metal ions<sup>22</sup>.

#### 3.4.2. Optimization

The experimental finding from the current density suggested that at low current density values, a high microhardness coating was obtained. This result is consistent with the research of Sachin<sup>16</sup>. Indeed, they were found that the charge transfer is easily achieved at low current densities which gives a nice coating.

It has been found that temperature plays an important role in the chemical composition and appearance of the deposits obtained. Indeed, the increase of this parameter has a negative effect on the quality and morphology of the coating. This finding is the same as that of Lotfi et al.<sup>18</sup> where a compact, non-cracking morphology was obtained at temperatures between 30-40°C.

#### 4. CONCLUSIONS

In order to protect ordinary steel against corrosion, the electrodeposition of a binary alloy composed of zinc and nickel was examined from a sulfate acid bath.

Based on the results of the mixture design, it can be concluded that the optimal values for the concentrations of boric acid, saccharin, and 2-butyne-1,4-diol are 0.1 M, 0.3g/L, and 0.1g/L respectively.

Summarizing the results obtained by applying the Box-Behnken design, it was found that the optimal operating conditions that improve the quality of the coating are: T= 30°C;  $i = 0.5A/dm^2$  and  $[Ni^{2+}]/[Zn^{2+}] = 0.53$  with a theoretical response of 312.66 HV and an experimental response of 312.30 HV.

From SEM and EDS analyses that have been carried out, it is possible to have several pieces of information about the electrocrystallization process, surface morphology, and mass percentage of the different constituents of the obtained coatings. It was found that the addition of the additives improved the quality of the coatings whose grain size became smaller in the presence of the two additives. In addition, the elemental analysis allowed us to observe that the thin film formed contains a high proportion of zinc, followed by nickel and some traces of oxygen.

#### ACKNOWLEDGEMENTS

We thank Dr. Farida BENDEBANE Director of the LOMOP Research Laboratory for providing us the software Minitab 19 and the necessary material resources. The authors thank also the Higher National School of Mines and Metallurgy-Amar Laskri, Algeria for the assistance provided in this research, represented in SEM analyzes.

#### Conflict of interests

*I declare that there is no a conflict of interest with any person, institute, company, etc.*

#### REFERENCES

1. Rashmi, D.; Pavithra, G. P.; Praveen, B. M.; Devapal, D.; Nayana, K. O.; Nagaraju, G. *Journal of Failure Analysis and Prevention*. **2020**, 20, 513-522.

2. Costa, J. M. ; de Almeida Neto, A. F. E. *Ultrasonics Sonochemistry*. **2021**, 73, 105495.

3. Hegde, A. C. ; Venkatakrishna, K.; Eliaz, N. *Surface and Coatings Technology*. **2010**, 205(7), 2031-2041.

4. Al-Murshedi, A. Y. ; Al-Rubaie, Z. F. *Annals of the Romanian Society for Cell Biology*. **2021**, 25(6), 4622-4633.

5. Hegde, A. C. ; Venkatakrishna, K. ; Eliaz, N. *Surface and Coatings Technology*. **2010**, 205(7), 2031-2041.

6. Maniam, K. K. ; Paul, S. *Applied Sciences*, **2020**, 10(15), 5321.

7. Gavrilă, M.; Millet, J. P.; Mazille, H.; Marchandise, D.; Cuntz, J. M. *Surface and coatings technology*, **2000**, 123(2-3), 164-172.

8. Tafreshi, M.; Allahkaram, S. R.; Farhangi, H. *Materials Chemistry and Physics*. **2016**, 183, 263-272.

9. Bories, C.; Bonino, J. P.; Rousset, A. *Journal of Applied Electrochemistry*. **1999**, 29, 1045-1051.

10. Arab, A.; Caceres, A.; Singh, R.; Eybel, R.; Medraj, M. In CSME Congress 2022, Proceedings of the Canadian Society for Mechanical Engineering International Congress 2022, Edmonton, AB, Canada, June 5-8, 2022.

11. Sun, H.; Wang, H.; Yang, S.; Xiaokou, S.; Zhou, X.; Wang, B.; Sun, J. *ChemistrySelect*. **2022**, 7(38), e202201899.

12. Bae, S. H.; Oue, S.; Taninouchi, Y. K.; Son, I.; Nakano, H. *isij international*. **2022**, 62(7), 1522-1531.

13. Cornell, J.A. *Experiments with Mixtures: Designs, Models and the Analysis of Mixture Data*, 3rd ed., Wiley, 2002.

14. Montgomery DC. *Design and Analysis of Experiments*, 7th ed. John Wiley and Sons, **2008**.

15. Tian, W.; Xie, F. Q.; Wu, X. Q.; Yang, Z. Z. *Surface and Interface Analysis: An International Journal devoted to the development and application of techniques for the analysis of surfaces, interfaces and thin films*. **2009**, 41(3), 251-254.

16. Sachin, H. P.; Achary, G.; Arthoba Naik, Y.; Venkatesha, T. V. *Bulletin of Materials Science*. **2007**, 30, 57-63.

17. Tsuru, Y.; Nomura, M.; Foulkes, F. R. *Journal of Applied Electrochemistry*. **2002**, 32, 629-634.
18. Lotfi, N.; Aliofkhazraei, M.; Rahmani, H.; Darband, G. B. *Protection of metals and physical chemistry of surfaces*. **2018**, 54, 1102-1140.
19. Shivakumara, S.; Manohar, U.; Arthoba Naik, Y.; Venkatesha, T. V. *Bulletin of Materials Science*. **2007**, 30, 455-462.
20. Othman, I. S.; Azam, M. A. F. M. M.; Shafie, M.; Kasim, M. S.; dan Pembuatan, F. T. K. M. *Proceedings of Mechanical Engineering Research Day*. **2020**, 357-358.
21. Riastuti, R.; Siallagan, S. T.; Rifki, A.; Herdino, F.; Ramadini, C. In *IOP Conference Series: Materials Science and Engineering*, IOP Publishing, Tangerang Selatan, Indonesia, September 25–26, 2018.
22. Nam, D. H.; Hong, K. S.; Kim, J. S.; Lee, J. L.; Kim, G. E.; Kwon, H. S. *Surface and Coatings Technology*. **2014**, 248, 30-37.